Linker effect of ferrocenylnaphthalene diimide ligands in the interaction with double stranded DNA

Shinobu Sato [a], Shigeori Takenaka [b,*]

[a] *Department of Bioscience and Bioinformatics, Kyushu Institute of Technology, Iizuka-shi, Fukuoka 820-8502, Japan*
[b] *Department of Applied Chemistry, Kyushu Institute of Technology, Kitakyushu-shi 804-8550, Japan*

Abstract

Ferrocenylnaphthalene diimide ligands **1–7** were synthesized by joining a piperazino or *N*-methylamino linker of the naphthalene diimide skeleton with ferrocenecarboxylic, ferroceneacetic, or ferrocenepropionic parts. Their interaction with double stranded DNA (dsDNA) was studied kinetically and electrochemically. Association rate constants of these ligands were found to correlate with their intramolecular stacking ability between the ferrocene and naphthalene diimide planes: ligands which can adopt a stacked conformation in buffer solution were unfavorable in the association with dsDNA, resulting in a smaller association rate constant. Dissociation rate constants of these ligands carrying the bulky piperazino linker were smaller than that of those carrying an *N*-methylamino one. Binding constants were dictated by the balance of these two factors. These ligands were applied to the electrochemical detection of the amount of dsDNA on the electrode. Ligand **6** having the highest affinity for dsDNA gave rise to the largest current increase upon dsDNA formation in the electrochemical hybridization assay.
© 2008 Elsevier B.V. All rights reserved.

Keywords: Ferrocenylnaphthalene diimide; Double stranded DNA; Binding parameter; Electrochemical gene detection

1. Introduction

Electrochemical gene analysis has attracting considerable attention from a standpoint of rapid and simple detection of genes with high sensitivity [1–18]. Electrochemical gene analysis has been done by the criteria to determine whether double stranded DNA (dsDNA) could be formed with sample DNA on the DNA probe-immobilized electrode. Several researchers have been developing the following methods to obtain a dsDNA formation signal electrochemically: (i) labeling of electrochemically active moieties to DNA sample and its hybridization with a DNA probe-immobilized electrode [1,2], (ii) immobilization of an electrochemically active DNA probe on the electrode and its electrochemical signal change after hybridization [3,4], (iii) impedance change before and after

hybridization with sample DNA [5,6], or (iv) detection of the electrochemical signal of the ligand bound to the dsDNA formed between sample DNA and probe DNA on the electrode [7–17]. The methods (i) and (ii) require labeling of the sample DNA with electrochemically active molecules, whereas methods (iii) and (iv) do not require such a labeling reaction especially in (iv). Electrochemical detection can be achieved simply by the addition of a ligand in (iv).

We have been developing ferrocenylnaphthalene diimide derivatives as ligand for dsDNA detection and are developing an electrochemical hybridization assay for electrochemical gene detection. Ferrocenylnaphthalene diimide can bind to dsDNA through threading intercalation to form a stable complex. The ferrocenyl linker chain of this ligand can act as an anchor to prevent its dissociation from dsDNA. At first, we reported the application of ferrocenylnaphthalene diimide (**1**) in the single nucleotide polymorphism (SNP) analysis of lipoprotein lipase [11,12] and

---
* Corresponding author. Tel./fax: +81 93 884 3322.
  E-mail address: shige@che.kyutech.ac.jp (S. Takenaka).

p53 genes [14]. In those studies, both PCR products and genomic DNA were amenable, but the redox potential of **1**, 0.45 V vs. Ag/AgCl, overlapped with the background current from the electrolyte used. To circumvent this problem, ferrocenylnaphthalene diimide (**5**) having a lower potential, was synthesized and its interaction with dsDNA was studied [15]. It turned out that the redox potential of **5** appeared at 0.28 V vs. Ag/AgCl, where the effect of the background current was negligible and that it has higher binding affinity for dsDNA than **1**. Encouraged by these observations, a series of ferrocenylnaphthalene diimide ligands **1–7** were designed and synthesized, and their binding behavior with dsDNA and the electrochemical response of the resulting complex on the electrode were studied systematically in this paper.

2. Experimental

2.1. General

Melting points are uncorrected. ^{1}H NMR spectra were recorded on a Bruker AC250P spectrometer operating at 250 MHz or Bruker AVANCE 400 spectrometer operating at 400 MHz for proton with tetramethylsilane (TMS) as an internal standard. Mass spectra (MS) were taken on a Voyager™ Linear-SA (PerSeptive Biosystems Inc., Foster city, CA) by the time-of-flight mode with α-cyano-4-hydroxy-cinnamic acid as matrix. Electronic absorption spectra were recorded with Hitachi 3300 spectrophotometers equipped with an SPR10 temperature controller.

Calf thymus DNA was purchased from Sigma–Aldrich (St. Louis, MO) and used after sonication according to the method reported previously [19]. The concentration of calf thymus DNA was estimated from the molar absorptivity based on nucleic bases of 6412 cm^{-1} M^{-1} at 260 nm [20]. Oligonucleotides, thiolated dT$_{20}$ (HS-dT$_{20}$) and dA$_{20}$, used in this study were custom synthesized by Genenet Co. (Fukuoka, Japan) and their concentrations were estimated from the molar absorptivities of 162 600 and 243 400 cm^{-1} M^{-1} at 260 nm, respectively.

2.2. Synthesis

Ferrocenylnaphthalene diimide derivatives **1–7** were synthesized according to the route given in Scheme 1.

Ferrocenepropionic acid was synthesized from trimethylamminomethylferrocene in 24% yield according to the procedure reported previously [21]. M.p. 119–121 °C (121–122 °C [21]); ^{1}H NMR (250 MHz, CDCl$_3$) δ 2.71–2.58 (4H, m) and 4.12–4.08 (9H, m) ppm. N,N'-bis[3-(3-ferroceneacetamidopropyl)methylaminopropyl]-naphthalene-1,4,5,8-tetracarboxylic acid diimide (**5**) was synthesized as a brown solid by the route previously reported [15]. M.p. 159–160 °C (M.p. 159–160 °C [15]). Ferrocenecarboxylic acid N-hydroxysuccinimide ester (**14**) was synthesized in 89% yield according to the procedure reported previously as an orange colored solid [22]; M.p. 161–163 °C; ^{1}H

NMR (250 MHz, CDCl$_3$) δ 2.88 (4H, s), 4.39 (5H, s), 4.57 (2H, t), and 4.94 (2H, d) ppm. N,N-bis[3-(3-aminopropyl)methylaminopropyl]naphthalene-1,4,5,8-tetracarboxylic acid diimide (**13**) was synthesized by the route reported previously [15]. N,N'-bis(3-ferrocenylamidomethylamino-propyl)-naphthalene-1,4,5,8-tetracarboxylic acid diimide (**7**) was synthesized by the route reported previously [23]. M.p. 191–193 °C (182–185 °C [23]).

### 2.2.1. Ferrocenepropionic acid N-hydroxysuccinimide ester (15)

A solution of ferrocenepropionic acid (0.56 g, 2.2 mmol) and N-hydroxysuccinimide (0.28 g, 2.4 mmol) in dioxane (9 ml) was added with stirring to a solution of dicyclohexylcarbodiimide (0.49 g, 2.4 mmol) in dioxane (15 ml) over a period of 1 h at 0 °C. The reaction was allowed to proceed for 16 h at room temperature. The precipitate formed was removed by filtration, and the filtrate was evaporated to leave a yellow solid. The crude product was purified by collecting the R_f = 0.10 (choloroform/hexane = 10:1) fraction on silica gel chromatography with the same solvent as eluent: yield: 0.50 g (64%); M.p. 117–119 °C. ^{1}H NMR (400 MHz, CDCl$_3$) δ 1.85 (t, J = 3.48 Hz, 2 H, FcCH$_2$-CH$_2$), 2.67–2.87 (m, 6H, FcCH$_2$CH$_2$ + CH$_2$ of Su), and 4.17–4.13 (m, 9H, CpH) ppm.

2.2.2. [3-[4-(3-Aminopropyl)piperazin-1-yl]propyl]-carbamic acid tert-butyl ester (8) [24]

N,N'-bis(3-Aminopropyl)piperazine (20.6 ml, 0.10 mol) was dissolved in dioxane (10 ml) and S-tert-butoxycarbonyl-4,6-dimethyl-2-mercaptopyrimidine (4.8 g, 20 mmol) in dioxane (50 ml) was added slowly to this solution with stirring. The precipitate formed during this time was taken up in a small amount of water. After stirring for 18 h, the precipitate remained was filtered off and the filtrate was evaporated. The residue was taken up in water (20 ml) containing 20 g of NaCl, and then extracted with ethyl acetate. The organic phase was combined, dried over potassium carbonate, and evaporated under reduced pressure to give **8** as yellow viscous oil: yield 5.3 g (88% for S-tert-butoxy-carbonyl-4,6-dimethyl-2-mercaptopyrimidine). ^{1}H NMR (400 MHz, CDCl$_3$) δ 1.28 (s, 9H, t-Bu), 1.60–1.68 (m, 4H, H$_2$NCH$_2$CH$_2$ + NHCH$_2$CH$_2$), 2.37–2.47 (m, 12H, CH$_2$N(CH$_2$CH$_2$)$_2$NCH$_2$), 2.74 (t, J = 6.8 Hz, 2H, H$_2$NCH$_2$), 3.18 (t, J = 5.9 Hz 2H, NHCH$_2$), and 5.49 (br s, 1H, NHCO) ppm.

2.2.3. N,N'-bis[[3-(3-tert-Butoxycarbonylaminopropyl)-piperazin-1-yl]propyl]- naphthalene-1,4,5,8-tetracarboxylic acid diimide (10)

Naphthalene-1,4,5,8-tetracarboxylic dianhydride (1.3 g, 5.0 mmol) and mono-Boc amine **8** (7.3 g, 24 mmol) were refluxed in THF (31 ml) for 18 h. The reaction mixture was allowed to cool and then poured into chloroform (50 ml). The precipitate formed was removed by filtration and the solvent was removed under reduced pressure. The residue was dissolved in methanol (30 ml) and poured
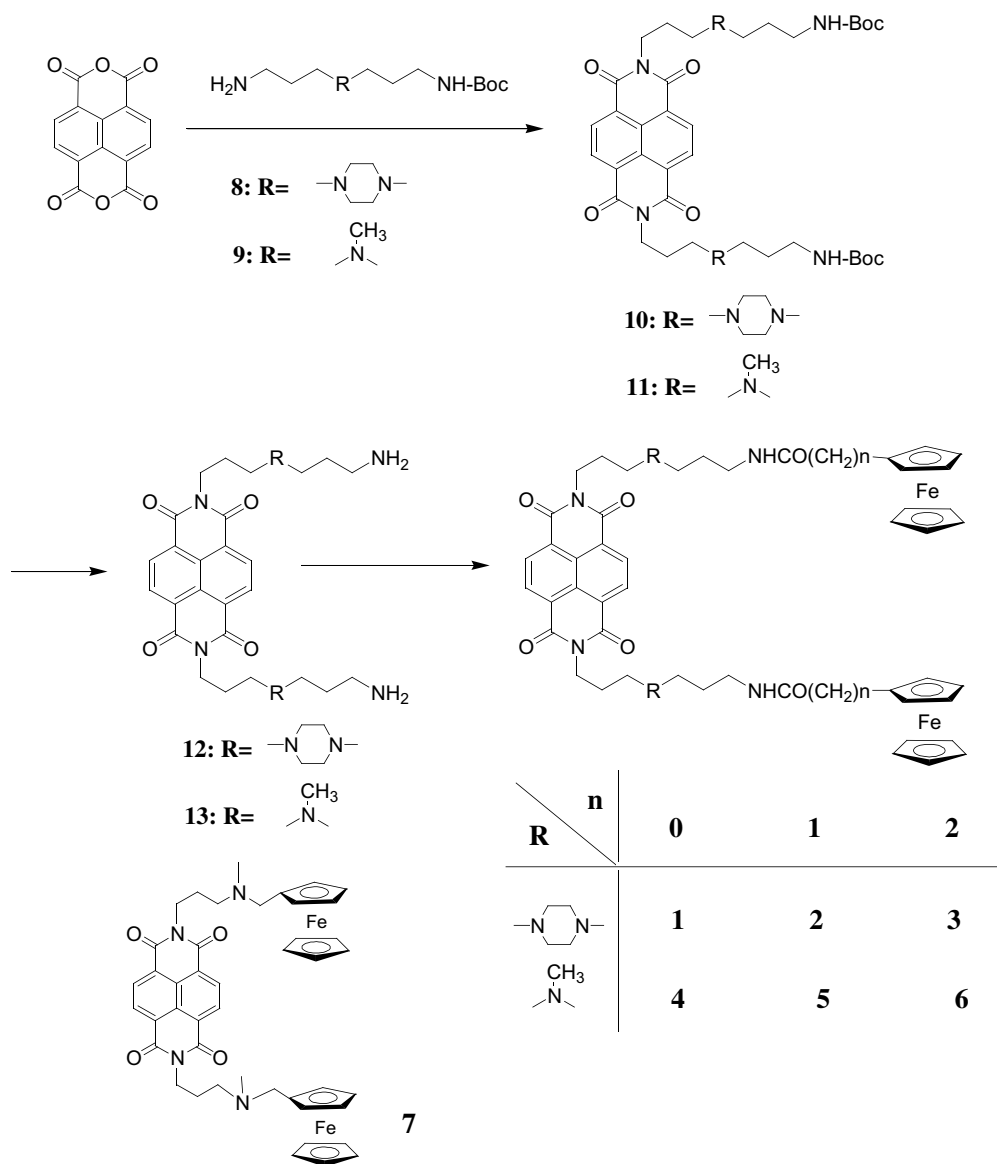
Scheme 1.

into water (200 ml). The product was obtained as a reddish brown solid: yield: 0.58 g (14%). M.p. 162–163 °C. ^{1}H NMR (400 MHz, CDCl$_3$) δ 1.42 (s, 18H, t-Bu), 1.61 (m, 4H, NHCH$_2$CH_2), 1.95 (m, 4H, NCH$_2$CH_2), 2.29 (m, 8H, CH_2N(CH$_2$CH$_2$)$_2$NCH_2), 2.50 (m, 8H, CH$_2$N(CH_2CH_2)$_2$NCH$_2$), 3.15 (m, 4H, NHCH_2), 4.28 (t, J = 7.0 Hz, 4H, NCH_2), and 8.76 (s, 4H, Ar–H) ppm. Elemental Anal. Calc. for C$_{44}$H$_{64}$N$_8$O$_8$: C, 63.44; H, 7.74; N, 13.45. Found: C, 63.17, H, 7.71; N, 4.69%.

2.2.4. N,N′-bis[[3-(3-Aminopropyl)piperazin-1-yl]propyl]-naphthalene-1,4,5,8-tetracarboxylic acid diimide (12)

Boc naphthalene diimide derivative **10** (0.58 g, 0.69 mmol) was dissolved in trifluoroacetic acid (TFA) (5 ml) and the solution was stirred for 40 min. TFA was removed under reduced pressure after addition of a small amount of methanol to obtain an pale brown solid. This solid was dissolved in methanol (30 ml) and poured into

chloroform (400 ml) and kept at 4 °C overnight. The precipitate formed was collected and dried under reduced pressure to leave a pale pink solid: yield: 0.69 g (70%). M.p. 180–181 °C. Elemental Anal. Calc. for C$_{34}$H$_{64}$-N$_8$O$_4$ · 6CF$_3$COOH · 1.3 H$_2$O: C, 41.22; H, 4.16; N, 8.36. Found: C, 41.18, H, 4.12; N, 8.6%.

2.2.5. N,N′-bis[[4-(3-Ferrocenecarboamidopropyl)piperazin-1-yl]propyl]-naphthalene-1,4,5,8-tetracarboxylic acid diimide (1)

Previously, **1** was synthesized with the amino group unprotected [10], but this route was switched to one, where the amino was protected with a Boc group to ease work-up and improve yield.

A solution of **12** (5.0 g, 3.8 mmol), **14** (3.1 g, 9.4 mmol), and triethylamine (5 ml) in chloroform (15 ml) was stirred at room temperature for 30 h and the solvent was removed. Chloroform (200 ml) was added, washed successively twice

each with saturated brine (200 ml each) and water (200 ml each), and dried over magnesium sulfate. The solvent was removed and the residue was chromatographed on silica gel (Merck 60) with methanol as eluent. The fraction showing a R_f of 0.2 on TLC (methanol) was collected and the solvent was removed under reduced pressure. The residue was dissolved in a small amount of methanol. The residue was taken up in a small amount of methanol, sonicated, and then the solvent evaporated. This process was repeated several times until the orange-yellow product (**1**) solidified: yield: 1.28 g (24%). M.p. 233–235 °C (M.p. 237–240 °C [10]). ^{1}H NMR (400 MHz, CDCl$_3$) δ 1.70 (m, 4H, NHCH$_2$CH_2), 1.97 (m, 4H, NCH$_2$CH_2), 2.40 (t, J = 6.2 Hz, 8H, CH_2N(CH$_2$CH$_2$)$_2$NCH_2), 2.55 (t, J = 6.9 Hz, 8H, CH$_2$N(CH_2CH$_2$)$_2$NCH$_2$), 3.44 (m, 4H, NHCH_2), 4.18 (s, 10H, CpH), 4.28 (m, 8H, COCCHCH of NHCOCp + NCH_2), 4.67 (d, J = 1.9 Hz, 4H, COCCHCH of NHCOCp), 7.00 (t, J = 5.7 Hz, 2H, NH) and 8.77 (s, 4H, Ar–H) ppm. MS m/z [M + H]$^+$ 1058.1 (theory for C$_{56}$H$_{64}$Fe$_2$N$_8$O$_6$ + H$^+$ 1057.9).

2.2.6. N,N′-bis[[4-(3-Ferroceneacetamidopropyl)piperazin-1-yl]propyl]-naphthalene-1,4,5,8-tetracarboxylic acid diimide (2)

A solution of **12** (0.60 g, 0.46 mmol), ferroceneacetic acid (0.26 g, 1.4 mmol), 1-ethyl-3-(3-dimethylaminopropyl-9-carbodiimide) (0.26 g, 1.4 mmol) and triethylamine (0.6 ml) in chloroform (3.7 ml) was stirred at room temperature for 27 h. The solvent was removed and the residue was chromatographed on silica gel with chloroform/methanol/diethylamine = 10/1.0/0.25 as eluent. The fraction showing an R_f of 0.4 on TLC with the same solvent was collected and the solvent was removed under reduced pressure. The residue was taken up in a small amount of methanol, sonicated, and then the solvent evaporated. This process was repeated several times until the yellow product (**2**) solidified: yield: 0.27 g (55%), M.p. 169–170 °C. ^{1}H NMR (400 MHz, CDCl$_3$) δ 1.85 (m, 4H, NHCH$_2$CH_2), 1.95 (m, 4H, NCH$_2$CH_2), 2.23 (t, J = 6.9 Hz, 8H, CH_2N(CH$_2$CH$_2$)$_2$NCH_2), 2.51 (t, J = 7.0 Hz, 8H, CH$_2$N(CH_2CH$_2$)$_2$NCH$_2$), 3.23 (m, 4H, NHCH_2), 3.27 (s, 4H, CH_2Cp) 4.10 (s, 10H, CpH), 4.13 (m, 8H, CH$_2$CCHCH of CH$_2$Cp + NCH_2), 4.27 (d, J = 7.2 Hz, 4H, CH$_2$CCHCH of CH$_2$Cp), 6.4 (t, J = 5.7 Hz, 2H, NH) and 8.75 (s, 4H, Ar–H) ppm. Elemental Anal. Calc. for C$_{58}$H$_{68}$Fe$_2$N$_8$O$_6$ · 0.8H$_2$O: C, 63.37; H, 6.31; N, 10.19. Found: C, 63.35, H, 6.26; N, 10.30%. MS m/z [M + H]$^+$ 1088.7 (theory for C$_{58}$H$_{68}$Fe$_2$N$_8$O$_6$ + H$^+$ 1085.9).

2.2.7. N,N′-bis[[4-(3-Ferrocenepropionamidopropyl)-piperazin-1-yl]propyl]-naphthalene-1,4,5,8-tetracarboxylic acid diimide (3)

A suspension of **12** (0.29 g, 0.22 mmol) in chloroform (10 ml) was dissolved by addition of triethylamine (0.19 ml, 1.3 mmol) and **15** (0.23 g, 0.65 mmol) was added and the mixture was stirred at room temperature for 18 h. Chloroform (50 ml) was added, washed with water

(50 ml), and dried over magnesium sulfate. The solvent was removed and the residue was chromatographed on silica gel with chloroform/methanol/diethylamine = 10/0.2/0.5 as eluent. The fraction showing an R_f of 0.25 on TLC with the same solvent was collected and the solvent was removed under reduced pressure. The residue obtained was taken up in a small amount of methanol, sonicated, and then the solvent evaporated. This process was repeated several times until the orange product (**3**) solidified: yield: 0.12 g (49%), M.p. 168–170 °C. ^{1}H NMR (400 MHz, CDCl$_3$) δ 1.58 (m, 4H, NHCH$_2$CH_2), 1.95 (m, 4H, NCH$_2$-CH_2), 2.28–2.23 (m, 12H, CH_2N(CH$_2$CH$_2$)$_2$NCH_2 + CH$_2$Cp), 2.51 (t, J = 6.9 Hz, 8H, CH$_2$N(CH_2CH$_2$)$_2$NCH$_2$), 2.68 (t, J = 7.3 Hz, 4H, COCH_2), 3.30 (m, 4H, CON-HCH_2) 4.02 (d, J = 1.7 Hz, 4H, CH$_2$CCHCH of CH$_2$Cp), 4.06 (d, 4H, CH$_2$CCHCH of CH$_2$Cp), 4.09 (s, 10H, CpH), 4.27 (t, J = 7.3 Hz, 4H, NCH_2), 7.03 (t, J = 4.8 Hz, 2H, NH) and 8.76 (s, 4H, Ar–H) ppm. Elemental Anal. Calc. for C$_{60}$H$_{72}$Fe$_2$N$_8$O$_6$ · 0.6H$_2$O: C, 64.13; H, 6.51; N, 9.97. Found: C, 64.09, H, 6.52; N, 9.94%. MS m/z [M + H]$^+$ 1113.6 (theory for C$_{60}$H$_{72}$Fe$_2$N$_8$O$_6$ + H$^+$ 1114.0).

2.2.8. N,N-bis[3-(3-Ferrocenecarboxamidopropyl)methyl-aminopropyl]-naphthalene-1,4,5,8-tetracarboxylic acid diimide (4)

A suspension of **12** (1.0 g, 1.0 mmol) in chloroform (13 ml) was dissolved by addition of triethylamine (1.0 ml, 7.2 mmol) and **14** (1.0 g, 3.1 mmol) was added and the mixture was stirred at room temperature for 42 h. Chloroform (100 ml) was added, washed with water (50 ml), and dried over magnesium sulfate. The solvent was removed and the residue was chromatographed on silica gel with chloroform/methanol/diethylamine = 10/0.2/0.5 as eluent. The fraction showing an R_f of 0.20 on TLC in the same solvent was collected and the solvent was removed under reduced pressure. The residue was taken up in a small amount of methanol, sonicated, and then the solvent evaporated. This process was repeated several times until the orange product (**4**) solidified: yield: 0.29 g (30%), M.p. 185–186 °C. ^{1}H NMR (400 MHz, CDCl$_3$) δ 1.76 (m, 4H, NHCH$_2$CH_2), 1.99 (m, 4H, NCH$_2$CH_2), 2.32 (s, 6H, NCH$_3$), 2.53 (t, J = 6.0 Hz, 4H, NHCH$_2$CH$_2$-CH_2), 2.58 (t, J = 7.0 Hz, 4H, NCH$_2$CH$_2$CH_2), 3.49 (t, J = 8.6 Hz, 4H, CONHCH_2), 4.15 (s, 10H, CpH), 4.29 (m, 8H, COCpH), 4.67 (t, J = 1.9 Hz, 4H, NCH_2), 7.15 (t, J = 5.0 Hz, 2H, NH) and 8.75 (s, 4H, Ar–H) ppm. Elemental Anal. Calc. for C$_{52}$H$_{60}$Fe$_2$N$_6$O$_6$: C, 63.44; H, 5.75; N, 8.88. Found: C, 63.29, H, 5.91; N, 8.94%. MS m/z [M + H]$^+$ 975.46 (theory for C$_{52}$H$_{60}$Fe$_2$N$_6$O$_6$ + H$^+$ 975.76).

2.2.9. N,N′-bis[3-(3-Ferrocenepropionamidopropyl)methyl-aminopropyl]-naphthalene-1,4,5,8-tetracarboxylic acid diimide (6)

A suspension of **12** (0.29 g, 0.3 mmol) in chloroform (15 ml) was dissolved by addition of triethylamine

(0.26 ml, 1.8 mmol) and **15** (0.31 g, 0.90 mmol) was added and the mixture was stirred at room temperature for 42 h. Chloroform (100 ml) was added, washed with saturated brine four times (50 ml each), and dried over MgSO$_4$. The solvent was removed and the residue was chromatographed on silica gel with chloroform/methanol/diethylamine = 10/0.2/0.5 as eluent. The fraction showing R_f of 0.20 on TLC with the same solvent was collected and the solvent was removed under reduced pressure. The residue was taken up in a small amount of methanol, sonicated, and then the solvent evaporated. This process was repeated several times until the orange product (**6**) solidified: yield: 0.21 g (70%), M.p. 91–93 °C. ^{1}H NMR (400 MHz, CDCl$_3$) δ 1.68 (m, 4H, NHCH$_2$CH_2), 1.85 (m, 4H, NCH$_2$CH_2), 2.22 (s, 6H, NCH$_3$), 2.40–2.48 (m, 12H, CH_2N(CH$_3$)-CH_2 + CH_2Cp), 2.70 (m, 4H, CH_2CH$_2$Cp), 3.37 (m, 4H, CONHCH_2), 3.95 (m, 4H, CH$_2$CCHCH of CH$_2$Cp), 4.03–4.06 (m, 14H, CpH + CH$_2$CCHCH of CH$_2$Cp), 4.22 (t, $J = 7.7$ Hz, 4H, NCH$_2$), 6.98 (t, $J = 5.6$ Hz, 2H, NH) and 8.71 (s, 4H, Ar–H) ppm. Elemental Anal. Calc. for C$_{54}$H$_{62}$Fe$_2$N$_6$O$_6$: C, 64.68; H, 6.23; N, 8.38. Found: C, 64.63, H, 6.32; N, 8.10%. MS m/z [M + H]$^+$ 1005.0 (theory for C$_{54}$H$_{62}$Fe$_2$N$_6$O$_6$ + H$^+$ 1003.8).

2.3. Binding kinetics

Kinetic experiments were performed with an SF-61 DX2 double mixing stopped flow system (Hi-Tech Scientific Inc., Salisbury, UK) equipped with a Lauda RF206 temperature controller. Single absorbance vs. time was collected in 10 mM morpholinoethanesulfonic acid (MES) buffer (pH 6.2) containing 1 mM EDTA and 0.10 M NaCl. Absorbance was measured at 383 nm, the wavelength where the absorption of naphthalene diimide derivatives is largest. Association rate constants of ligands with dsDNA were obtained by fitting the exponential data of absorption change after mixing with a 10-fold excess of dsDNA over ligand to the equation of $A_1\exp(-k_1t) + A_2\exp(-k_2t)$, where A and k refer to the fractional amplitudes and rate constants, respectively, for the two-exponential fit to the results. Intrinsic second-order association rate constant (k_a) and dissociation rate constants (k_d) were obtained from the slope of the plot of apparent association rate constant (k_{app}) against dsDNA concentration according to the equation $k_{app} = k_a[DNA] + k_d$ [25]. Dissociation rate constant (k_d) of the ligand from dsDNA was determined by sodium dodecyl sulfate (SDS)-driven dissociation measurements described previously [26]. Two kinds of solutions (1% SDS and DNA–ligand complex) were mixed instantaneously using a piston and the change in the absorption spectrum was measured soon after mixing. Thus, when the DNA–ligand complex was mixed with an SDS solution, free ligand is incorporated into the SDS micelle. Since this process is diffusion-controlled, the entire absorption change represents the k_d-dependent process and therefore fitting of the kinetic trance provides k_d values.

2.4. Preparation of a 6-mercaptohexanol (6-MH)- or dT$_{20}$-immobilized electrode and hybridization of the latter with dA$_{20}$

A gold electrode (2.0 mm^2 in area) was polished with 6 μm, 1 μm of a diamond slurry, and 0.05 μm of an alumina slurry in this order and washed with Milli-Q water. The electrode was electrochemically polished by scanning 40 segments from −0.2 to 1.5 V at a scan rate of 100 mV/s in 0.5 M H$_2$SO$_4$ aqueous solution and washed with Milli-Q water. Masked electrodes were prepared by soaking the pretreated bare electrode in 100 μl of 1 mM 6-mercaptohexanol (6-MH) and subsequently incubating at 45 °C for 1 h and washing with Milli-Q water. dT$_{20}$-Immobilized electrodes were prepared by soaking the pretreated bare electrode in 100 μl of a 0.5 M NaCl solution containing HS-dT$_{20}$ (0.50 pmol/μl), keeping at 37 °C overnight, washing with Milli-Q water, and soaking in 100 μl of 1 mM 6-MH for 1 h at 45 °C. Hybridization with dA$_{20}$ was carried out by soaking the dT$_{20}$-immobilized electrode in 100 μl of 2.5 pmol/μl dA$_{20}$ in 2×SSC, 0.03 M sodium citrate buffer containing 0.3 M NaCl for 1 h at 25 °C.

2.5. Electrochemical measurements

Electrochemical measurements were carried out with an ALS model 600 electrochemical analyzer (CH Instrument, Austin, TX). Cyclic voltammogram (CV) and differential pulse voltammogram (DPV) were measured at 25 °C with a three-electrode configuration consisting of an Ag/AgCl reference electrode, a Pt counter electrode, and a dT$_{20}$-immobilized electrode before and after hybridization with dA$_{20}$ as working electrode in 0.10 M AcOK–AcOH buffer (pH 5.5) containing 0.10 M KCl and 50 μM ligand.

3. Results and discussion

3.1. Kinetic analysis

When ligands **1**–**7** were mixed with calf thymus DNA, the absorption at 383 nm decreased dramatically and underwent a slight bathochromic shift. This phenomenon is typical for threading intercalation of substituted naphthalene diimides into DNA and it was used for kinetic analysis of DNA interaction of these ligands [21,22]. A typical example of the association and dissociation kinetic traces for calf thymus DNA–**1** interaction is shown in Figs. 1 and 2. All data were analyzed by two-exponential fitting and the results determined for several ligands in 10 mM MES and 1 mM EDTA (pH 6.2) containing 0.10 M NaCl are summarized in Table 1. Binding constants calculated by dividing k_a by k_d and the molar absorptivities for these ligands in chloroform and buffer were also compiled in Table 1. The k_a value of **3** could not be determined because of precipitation upon mixing DNA and **3**.

Association rate constants for the ligands **1**–**6** increased in the following order: ferrocenepropionic (**3**) > ferrocene-
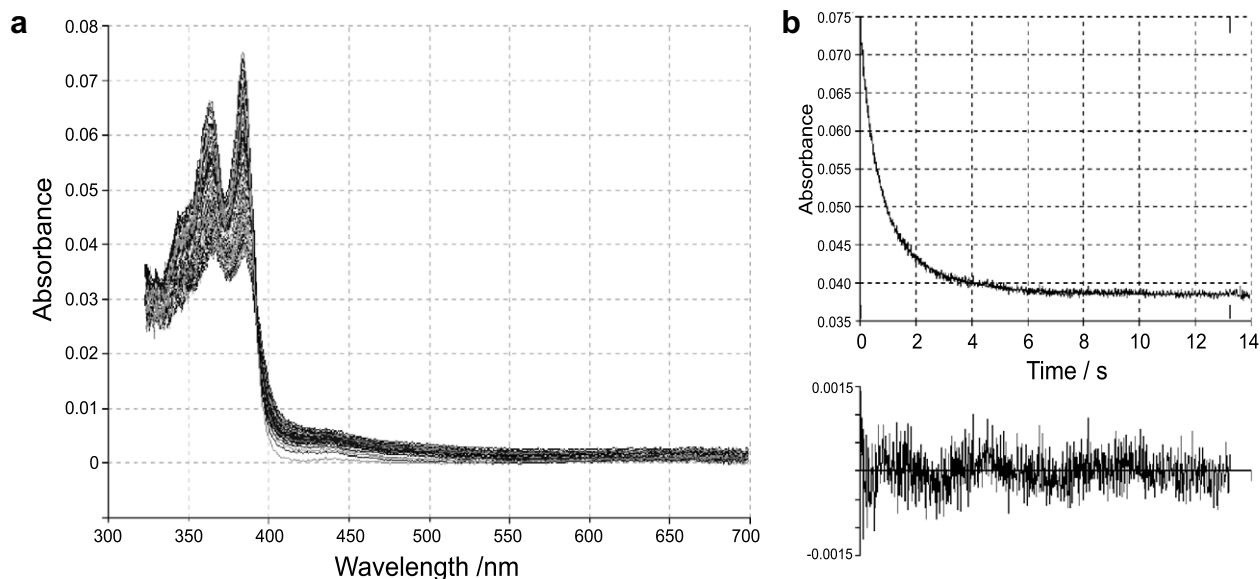
Fig. 1. Stopped-flow kinetic traces of absorption spectra (a) and absorption at 383 nm (b) for association of 10 μM **1** with 100 μM calf thymus DNA in 10 mM MES (pH 6.2) and 1 mM EDTA at 25 °C. Shown below the experimental plot are the residuals for the fit.
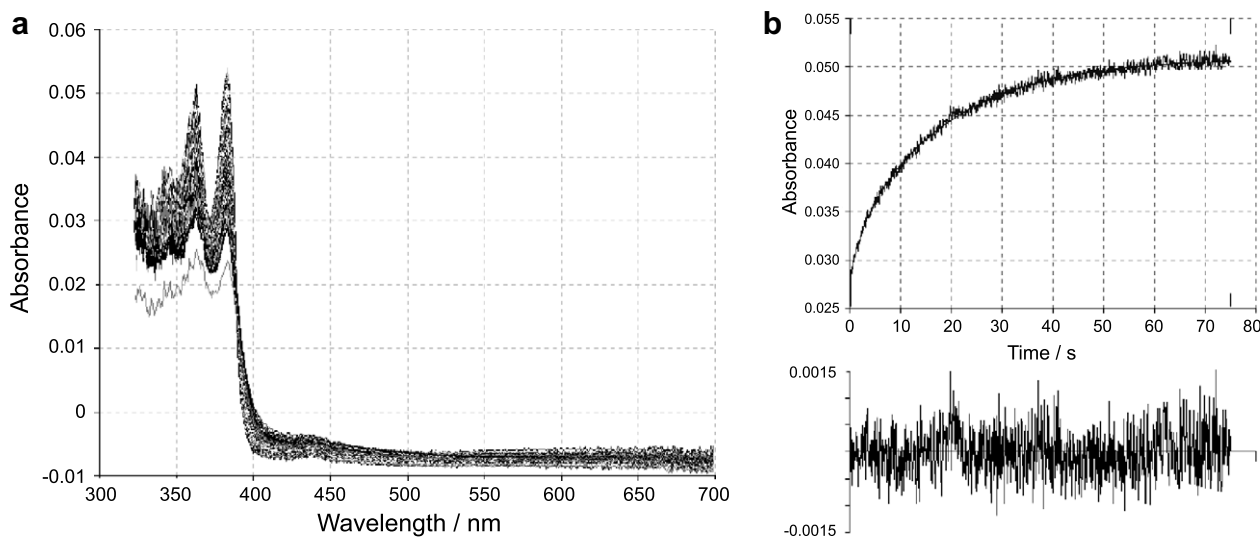

Fig. 2. Stopped-flow kinetic traces of absorption spectra (a) and absorption at 383 nm (b) for SDS-driven dissociation of 10 μM **1** from 100 μM calf thymus DNA in 10 mM MES (pH 6.2) and, 1 mM EDTA at 25 °C. Shown below the experimental plot are the residuals for the fit.

acetic (**2,5**) > ferrocenecarboxylic types of ligands (**1,4**). Molar absorptivities of the ligands in chloroform and 10 mM MES and 1 mM EDTA (pH 6.2) containing 0.10 M NaCl were about $3 \times 10^4 \, \text{cm}^{-1} \, \text{M}^{-1}$, and those in the buffer increased in the following order: ferrocenecarboxylic (**1**, **4**) > ferroceneacetic (**2,5**) > ferrocenepropionic type ligands (**3**, **6**). This order correlates with that of association rate constant. This coincidence stems presumably from the fact that the decreased molar absorptivity in the buffer should derive from the intramolecular stacking between the ferrocene and naphthalene diimide parts. As the stacked conformation of the ligands in the buffer should be transformed to an extended one upon threading intercalation into dsDNA, these ligands were not favorable in the association with dsDNA. On the other hand, disso-

ciation rate constants of the N-methylamino linker type ligands (**1–3**) were smaller than that of piperazino linker type ligands (**4–6**). Although the piperazino linker has larger molecular size than the N-methylamino one, the piperazino linker should act as an effective anchor to prevent dissociation from dsDNA.

Binding constants, Ks, were calculated from the k_a and k_d values, and the Ks values thus obtained increased as follows: **4** < **5** < **7** < **2** < **1** < **6**. The binding constants of the piperazino type ligands (**1–3**) were larger than those of the N-methylamino type ligands (**4–6**). The binding constants of these ligands seem to be dictated by the balance between the ease of threading into dsDNA and the stability of the dsDNA–ligand complex. The latter factor was the main determinant of the binding constant.

Table 1
Binding parameters and molar absorptivities of **1**–**7**[a]

Ligand	$10^{-4}k_a$ ($M^{-1}\,s^{-1}$)	k_d (s^{-1})	10^{-4} K (M^{-1})	$10^{-4}\varepsilon$ ($cm^{-1}\,M^{-1}$)	
				In chloroform	In buffer
1	2.35	0.13	18.1	3.1	2.6
2	5.50	0.42	13.0	3.1	2.9
3	[b]	1.32		3.1	2.8
4	2.34	1.82	1.28	2.8	2.4
5	5.61	0.84	6.70	3.1	2.6
6	153	1.75	87.4	2.9	3.0
7	14.1	1.34	10.5	3.0	2.4

[a] Unless stated otherwise, experiments were conducted in 10 mM MES (pH 6.2) and 1 mM EDTA containing 0.10 M NaCl at 25 °C.
[b] Data were not obtained because of low solubility of **3**.

3.2. Electrochemical behavior

Cyclic voltammograms (CVs) were measured with a gold electrode in 0.10 M AcOK–AcOH buffer (pH 5.5) containing 0.10 M KCl and 50 μM ligands **1**–**7**. As the observed redox response derives from the ligand absorbed on the gold electrode, CVs were measured with the 6-MH-immobilized electrode in the same electrolyte to suppress this absorption. Examples of CVs and differential pulse voltammograms (DPVs) of **1**–**7** are shown in Fig. 3. A one-step redox reaction of the ferrocene moiety of **1**–**7** were observed over 0.18–0.44 V as shown in Table 2. The piperazino linker type ligands (**1**–**3**) gave rise to $E_{1/2M}$ at the more positive sides than the N-methyl linker type ligands (**4**–**6**). $E_{1/2M}$s for ferrocenecarboxylic, ferroceneacetic, ferrocenepropionic type ligands decreased in this order. This is reasonable, given the electron-donating ability of the substituent attached to the ferrocene skeleton. ΔE_{pM}s of these ligands were about 60 mV. The oxidative peak current, i_{pa}, was plotted against the logarithm of the scan rates for the individual peaks of these ligands, and the slope obtained (0.51–0.75) suggests that the absorption process contributes partially to the electron transfer reaction in these cases.

The electrochemical parameters for **1**–**7** with a $dA_{20}dT_{20}$-immobilized electrode are also summarized in Table 2. $E_{1/2D}$s slightly shifted towards the positive side in this case. ΔE_{pD}s were also slightly smaller than those in the modified electrode. Furthermore, these slopes of the logarithm of the scan rate for the individual peak current were in the range of 0.77–0.96, which are larger than that in the modified electrode. These results suggested that the electrochemical signals are generated from the ligand intercalated into dsDNA on the electrode.

3.3. Electrochemical behavior of ligands in the DNA-immobilized electrode

To evaluate the preference of the ligands for dsDNA over ssDNA, DPVs of a dT_{20}- or $dA_{20}dT_{20}$-immobilized electrode were determined in the electrolyte containing
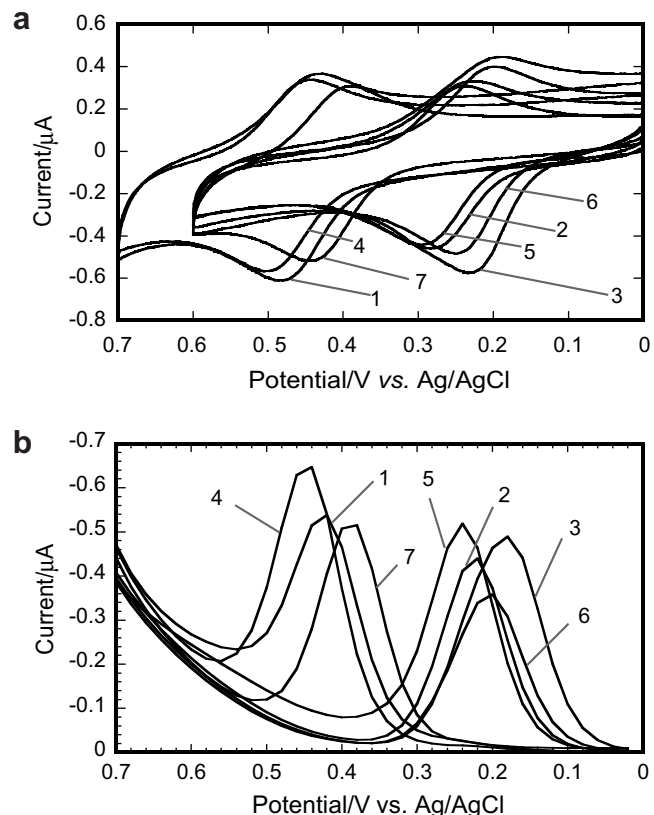

Fig. 3. Cyclic voltammograms (a) and different pulse voltammograms (b) for 50 μM **1**, **2**, **3**, **4**, **5**, **6**, and **7** on a 6-mercaptohexanol-immobilized gold electrode in 0.10 M AcOH–AcOK (pH 5.6) and 0.10 M KCl at 25 °C. Scan rate 100 mV/s.

Table 2
Electrochemical parameters for **1**–**7**[a]

Ligand	$E_{1/2M}$ (V)	ΔE_{pM} (V)	Slope$_M$	$E_{1/2D}$ (V)	ΔE_{pD}/V	Slope$_D$
1	0.45	0.61	0.61	0.47	0.29	0.77
2	0.25	0.59	0.63	0.26	0.29	0.92
3	0.21	0.46	0.75	0.23	0.41	0.96
4	0.47	0.61	0.51	0.47	0.35	0.79
5	0.26	0.60	0.60	0.27	0.31	0.84
6	0.22	0.55	0.66	0.23	0.34	0.91
7	0.41	0.57	0.62	0.41	0.36	0.80

[a] Experiments were conducted in 0.10 M AcOK–AcOH buffer (pH 5.6) and 0.10 M KCl containing 50 μM ligand at 25 °C. The can rate was 100 mV/s. Subscript M or D represents the experimental values in the case of 6-mercaptohexanol- or $dA_{20}dT_{20}$-immobilized electrodes, respectively. Slopes were obtained from the log–log plots of the oxidation peak current versus scan rate.

50 μM ligands. The DPV curves for **6** before and after hybridization of dA_{20} with a dT_{20}-immobilized electrode are shown in Fig. 4. A current peak of 2.0 μA was observed with the former electrode and the peak current increased to 5.1 μA after hybridization with dA_{20}. Current increases of similar magnitude were observed also for other ligands after hybridization as shown in Fig. 5. All data were standardized using Δi values, defined as $(i/i_o - 1) \times 100\%$, where i_o and i refer to the current before and after hybrid-
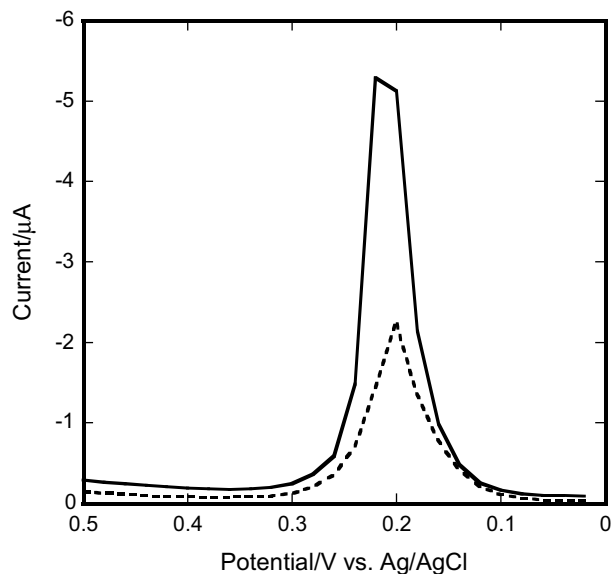
Fig. 4. Differential pulse voltammograms of a dT_{20}-immobilized gold electrode before (broken line) and after (solid line) hybridization with dA_{20} in 0.10 M AcOH–AcOK (pH 5.6), 0.10 M KCl, 50 μM **6** at 25 °C.

ization, respectively. The Δi values of these ligands were found to be 60–150%. Similar i_o or i values were obtained for **1–3**. However, when the individual data were scrutinized more closely, they were found to be in the following
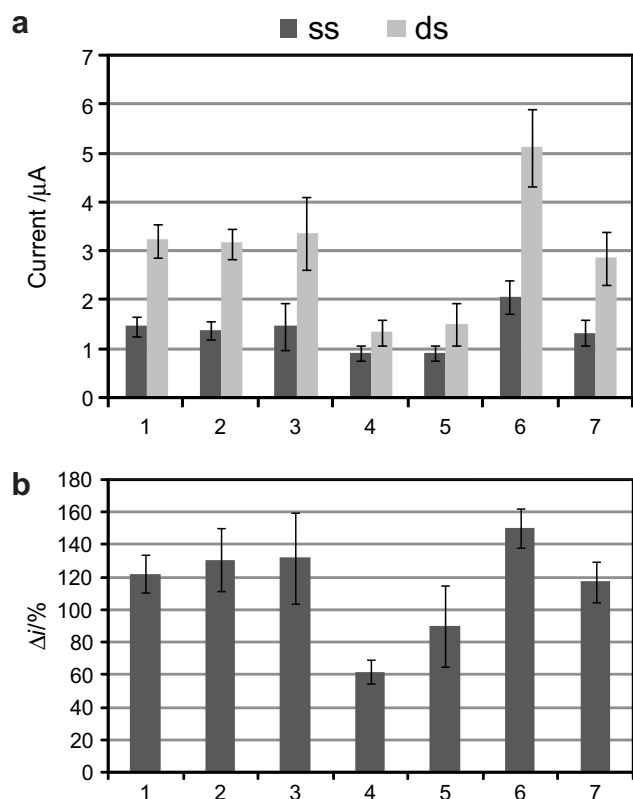

Fig. 5. (a) Current response for a dT_{20}-immobilized electrode before (i_o) and after (i) hybridization with dA_{20} in 0.10 M AcOK–AcOH (pH 5.6) and 0.10 M KCl containing 50 μM **1–7** at 25 °C. The number of measurements (n) = 6. Current change, Δi, defined as ($i/i_o - 1$) × 100% is also shown in (b).

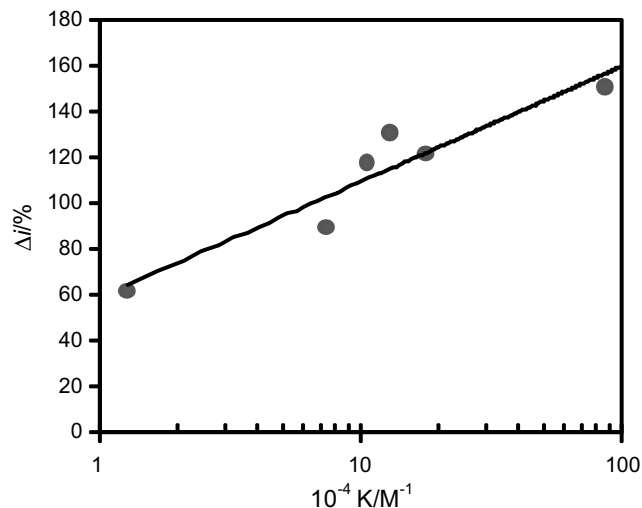Fig. 6. Correlation of the current increase after hybridization (Δi) against K.

order: **1** < **2** < **3** and the Δi values were also in the same order. A largest i value was obtained with **6**, while its i_o value was similar to those of other ligands, resulting in the largest Δi value for **6**. Ligands **4** and **5** showed smaller i_o and i values than other ligands for unknown reasons. Δi values of **4-6** were the following order: **4** < **5** < **6**. The Δi value of **7** was intermediate between the piperazino types (**1–3**) and the N-methylamino one excepting **6** (**4** and **5**). It was found that there is a good correlation between the Δi values and the K values (Fig. 6), suggesting that the current increase is based on the stability of the complex of ligand with dsDNA on the electrode. Although a k_a value for ligand **3** could not be determined, the K value may be estimated as 2.0×10^6 M^{-1} from Fig. 6.

4. Conclusion

Ferrocenylnaphthalene diimide ligands **1–7** synthesized in this paper gave rise to a redox peak current at various potentials (0.18–0.44 V), depending on the nature of the linker part of the ferrocene moiety. The binding affinity for dsDNA of these ligands also varied considerably (1.3×10^4–8.7×10^5 M^{-1}) depending on the linker chain. These values were found to correlate with the current increase after hybridization on the electrode. Ligand **6** having the highest affinity for dsDNA gave the current peak at 0.20 V, where the background current was smallest, and therefore **6** is the ligand most suitable for the electrochemical hybridization assay.

References

[1] R.M. Umek, S.W. Lin, J. Vielmetter, R.H. Terbrueggen, B. Irvine, C.J. Yu, J.F. Kayyem, H. Yowanto, G.F. Blackburn, D.H. Farkas, Y.-P. Chen, J. Mol. Diag. 3 (2001) 74–84.

[2] K. Mukumoto, T. Nojima, S. Sato, M. Waki, S. Takenaka, Anal. Sci. 23 (2007) 115–119.

[3] M. Inouye, R. Ikeda, M. Takase, T. Tsuji, J. Chiba, Proc. Natl. Acad. Sci. USA 102 (2005) 11606–11610.

[4] C.E. Immoos, S.J. Lee, M.W. Grinstaff, ChemBiochem 5 (2004) 1100–1103.

[5] Y.-T. Long, C.-Z. Li, T.C. Sutherland, H.-B. Kraatz, J.S. Lee, Anal. Chem. 76 (2004) 4059–4065.

[6] S. Pan, L. Rothberg, Langmuir 21 (2005) 1022–1027.

[7] A.K. Boal, J.K. Barton, Bioconjugate Chem. 16 (2005) 312–321.

[8] S.O. Kelley, J.K. Barton, N.M. Jackson, M.G. Hill, Bioconjugate Chem. 8 (1997) 31–37.

[9] K.M. Millan, S.R. Mikkelsen, Anal. Chem. 65 (1993) 2317–2323.

[10] S. Takenaka, K. Yamashita, M. Takagi, Y. Uto, H. Kondo, Anal. Chem. 72 (2000) 1334–1341.

[11] K. Yamashita, A. Takagi, M. Takagi, H. Kondo, Y. Ikeda, S. Takenaka, Bioconjugate Chem. 13 (2002) 1193–1199.

[12] T. Nojima, K. Yamashita, A. Takagi, M. Takagi, Y. Ikeda, H. Kondo, S. Takenaka, Anal. Sci. 19 (2003) 79–83.

[13] T. Nojima, K. Yamashita, A. Takagi, Y. Ikeda, H. Kondo, S. Takenaka, Anal. Sci. 21 (2005) 1437–1441.

[14] H. Miyahara, K. Yamashita, M. Kanai, K. Uchida, M. Takagi, H. Kondo, S. Takenaka, Talanta 56 (2002) 829–835.

[15] S. Sato, S. Fujii, K. Yamashita, M. Takagi, H. Kondo, S. Takenaka, J. Organomet. Chem. 637–639 (2001) 476–483.

[16] E.L.S. Wong, J.J. Gooding, Anal. Chem. 75 (2003) 3845–3852.

[17] K. Hashimoto, K. Ito, Y. Ishimori, Anal. Chem. 66 (1994) 3830–3833.

[18] M.R. Gore, V.A. Szalai, P.A. Ropp, I.V. Yang, J.S. Silverman, H.H. Thorp, Anal. Chem. 75 (2003) 6586–6592.

[19] M.W. Davidson, B.G. Griggs, D.W. Boykin, W.D. Wilson, J. Med. Chem. 20 (1977) 1117–1122.

[20] W. Muller, D.M. Crothers, Eur. J. Biochem. 54 (1975) 267–277.

[21] A. Anne, B. Blanc, J. Moiroux, Bioconjugate Chem. 12 (2001) 396–405.

[22] S. Takenaka, Y. Uto, H. Kondo, T. Ihara, M. Takagi, Anal. Biochem. 218 (1994) 436–443.

[23] S. Sato, T. Nojima, M. Waki, S. Takenaka, Molecules 10 (2005) 693–707.

[24] G.L. Stahl, R. Walter, C.K. Smith, J. Org. Chem. 43 (1978) 2285–2286.

[25] F.A. Tanious, S.-F. Yen, W.D. Wilson, Biochemistry 30 (1991) 1813–1819.

[26] S.-F. Yen, E.J. Gabbay, W.D. Wilson, Biochemistry 21 (1982) 2070–2076.